

# Performance Evaluation of Self-Compacting Concrete Containing Ceramic Waste Tile Fine Aggregate in Aggressive Environments

Research Paper Published: 03 February 2024

Volume 48, pages 3955–3970, (2024) Cite this article

[Download PDF](#) ↓

Access provided by Swami Keshvanand Institute of Technology Management and Gramothan



**Iranian Journal of Science and  
Technology, Transactions of Civil  
Engineering**

[Aims and scope](#)[Submit manuscript](#)

## Sanchit Anand

Department of Civil Engineering,  
Manipal University Jaipur, Jaipur,  
303007, India

[View author publications](#)

You can also search for this author  
in

[PubMed](#) | [Google Scholar](#)

[Ram Vilas Meena](#) ✉, [Abhishek Jain](#) ✉, [Ankit Singh Beniwal](#) ✉, [Om Prakash Singh](#) & [Sanchit Anand](#)

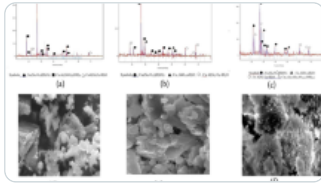
[133](#) Accesses [1](#) Citation [Explore all metrics](#) →

## Abstract

Self-compacting concrete (SCC) needs a massive extent of natural fine aggregate, which is affecting the river ecosystems due to the nonstop over-mining of it. Researchers are continuously working to decrease the dependence on natural fine aggregates and looking for green substitute materials. Hence, in this study, using ceramic wastes in SCC to replace fine aggregate will lead to a green environment and find proper ways to reduce waste disposal problems. This research aims to assess the systematic performance of SCC in an acidic environment by introducing up to 100% ceramic waste tile aggregate (CWTA) as a replacement for fine aggregates. Performance of SCC was evaluated by sulphate attack, chloride penetration, corrosion attack, carbonation, compressive strength, static and dynamic modulus of elasticity, scanning electron microscope (SEM), Fourier transform infrared (FTIR) and energy dispersive spectroscopy (EDS) tests. Outcomes indicated that incorporating up to 100% CWTA provided higher compressive strength and modulus of elasticity. All CWTA-based SCC mixes also showed superior resistance to chloride penetration, carbonation, corrosion and sulphate attack. Furthermore, the increment in replacement level after 60% has reduced most of the characteristics. However, mixes prepared with 80 and 100% CWTA also performed better than the control mix. It was noticed through SEM and EDS analyses that a considerable amount of hydration products

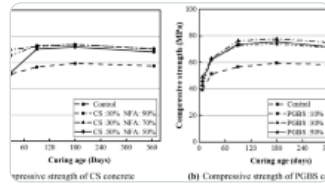
were developed in CWTA-based SCC, which confirmed the reason for the better performance of this mix compared to conventional SCC. Besides, FTIR analysis noticed the lower decay of portlandite and calcium silicate hydrate (CSH) gel for CWTA-based SCC mixes, which might cause higher resistance for them against sulphate attack. Incorporating up to 60% CWTA can thus be recommended as a feasible substitute to fine aggregate in SCC structures subjected to harsh environments.

## Similar content being viewed by others



### Durability performance of self-compacting concrete using binary and ternary blended pozzolanic and waste material

Article | 21 September 2023



### Study on Durability Properties of Sustainable Alternatives for Natural Fine Aggregate

Article | 24 September 2021



### Toxicity Characteristics and Heavy Metals Leachability of Self-Compacted Concrete Containing Fly Ash and Bottom Ash as Partia...

Chapter | © 2021

[Use our pre-submission checklist →](#)

Avoid common mistakes on your manuscript.



## 1 Introduction

Self-compacting concrete (SCC), which has better fresh properties and superior durability, has been gaining popularity in recent years. In 1980, Japanese researchers created SCC for the first time to reduce the construction's cost and time (Okamura et al. [2000](#)). The primary goal of SCC is to provide a homogeneous flowable mix without segregation, which can only be fulfilled by using a large content of powder or fine aggregate (Choudhary et al. [2021a](#)). However, the Indian Government has limited river sand mining due to severe environmental hazards (Jain et al. [2019](#)). The shortage of natural river sand has generated problems for the emergent concrete industry (Gupta and Siddique [2020](#)). The higher demand for fine aggregate is challenging for the world (Meena et al. [2023a](#)). Thus, the search for a sustainable alternative to natural resources is being worked on by researchers worldwide.

It is also stated that concrete structures are generally built for at least 50 years (Meena et al. [2021](#)). However, they are often impaired before their lifespan due to acidic environments such as chloride attack, corrosion, carbonation, and sulphate attack. Penetration of ions externally through soil, groundwater, and seawater into concrete structures develops harsh environments and ultimately triggers their deterioration (Jain et al. [2022a](#)). As the rate of deterioration increases, occasional replacement or repair of completely damaged concrete structures becomes essential, which is the most expensive and creates numerous social problems (Dezhampanah et al. [2020](#)). Earlier researchers have recommended using various industrial by-products as an alternative to natural aggregate for improving resistance against the harsh environment of concrete structures (Choudhary et al. [2021a](#); Chouhan et al. [2019](#); Gautam et al. [2022c](#); Jain et al. [2020a](#)). This study is,

hence, intended to assess the systematic behaviour of SCC subjected to the aggressive environment by using up to 100% ceramic waste tile aggregate (CWTA) as a replacement for fine aggregates.

## 2 Literature Review

---

Ceramics is a worldwide decorative being exploited on walls, floors, sanitary ware, sculptures, interiors, etc. On the other hand, ceramic industries are continuously rejecting large amounts of non-standard tiles during processing and quality control (Vilas Meena et al. [2021](#)). Another reason that adds to waste ceramic is transportation and fixing processing. About 30% of India's ceramic production was reportedly wasted by the ceramics sector (Gautam et al. [2022a](#)). This bulk quantity of ceramic waste creates environmental problems (Vilas et al. [2022b](#)). However, researchers worldwide reported that concrete containing ceramic waste resulted in better strength and durability properties and improved microstructure (Gautam et al. [2022b](#); Meena et al. [2023b](#); Siddique et al. [2018a](#)). Jerônimo et al. ([2018](#)) examined the corrosive behaviour of ground clay bricks incorporated with SCC. They stated that up to 20–30% replacement of cement with waste ground clay bricks enhanced the resistance to corrosion of the SCC mixture. Huseien et al. ([2020](#)) detected that incorporating ceramic tile waste powder (0–80% at 10% intervals) enhanced the fresh characteristics of self-compacting alkali-activated concrete. The concrete displayed excellent hardened state properties on incorporating ceramic tile waste powder. Gonzalez-Corominas and Etxeberria ([2014](#)) tested hardened characteristics of concrete made with ceramic waste as a substitution of up to 30% fine aggregate. They reported that compressive strength and flexural strength increased on substitution of up to 30% fine aggregate with ceramic waste. Medina et al. ([2013](#)) revealed that the water resistance behaviour of concrete was enhanced by replacing up to 25% recycled sanitary ware with coarse aggregate. Suzuki et al. ([2009](#)) examined the consequences of ceramic porous aggregates on autogenous shrinkage of concrete. The authors substituted the coarse aggregate with ceramic porous coarse aggregates at 10, 20, 30 and 40%. They observed the minimum shrinkage after the 40% substitution of ceramic porous in concrete. Higashiyama et al. ([2015](#)) investigated the influence on mortar behaviour of substituting natural river sand by waste ceramic aggregate produced by grinding and crushing electric porcelain insulator wastes. Meena et al. ([2023b](#)) assessed acid resistance performance of SCC incorporating waste ceramic as a replacement up to 100% of natural fine aggregate. They noticed the minimum loss of compressive strength and weight after 180 days of contact with sulphuric acid solution at up to 60% replacement level. Muniandy et al. ([2018](#)) studied viability of recycled waste ceramic in hot mix asphalt as aggregate substitution. The outcomes show that the resilient modulus strength and Marshall stability of the recycled waste ceramic hot mix asphalt mixes increased with 20% replacement.

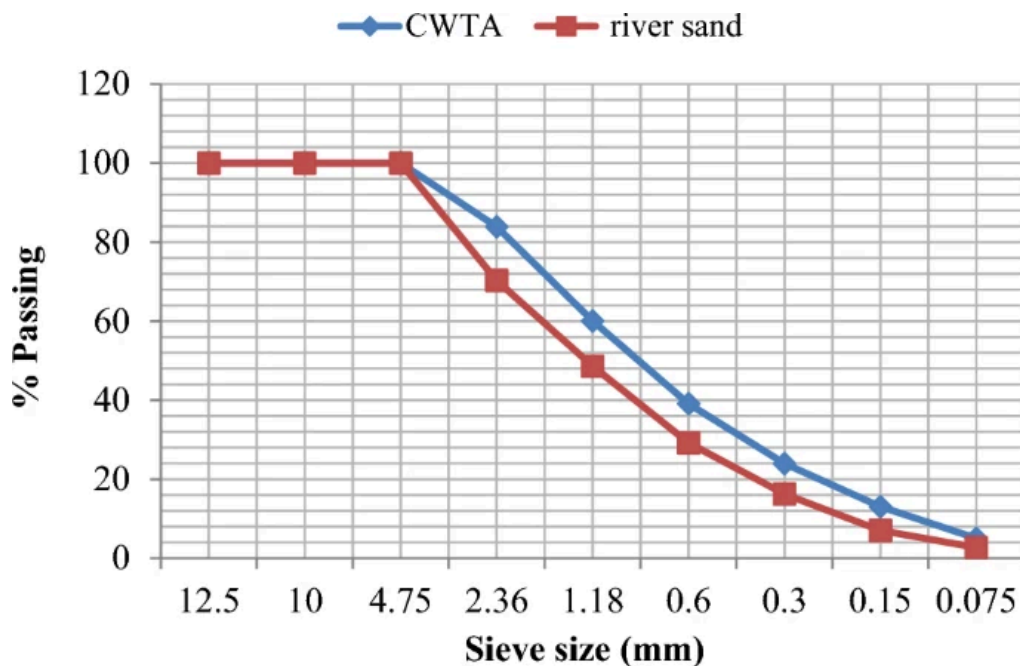
This research intends to systematically assess the SCC prepared with CWTA on exposure to harsh environments. Earlier, fresh characteristics of CWTA-based SCC mixtures have been calculated (Vilas et al. [2022a](#)). In this study, the durability and mechanical properties of SCC were assessed for sulphate attack, chloride penetration, corrosion attack, carbonation, compressive strength, and static and dynamic modulus of elasticity. Fourier transform infrared (FTIR), scanning electron microscope (SEM), and energy dispersive spectroscopy (EDS) were performed to examine the microstructural behaviour of SCC. Test results can confirm the reliability of CWTA as an SCC component in a harsh environment. This study could help to reduce the environmental effect of SCC by decreasing natural fine aggregate utilization.

## 3 Materials and Methods

### 3.1 Materials

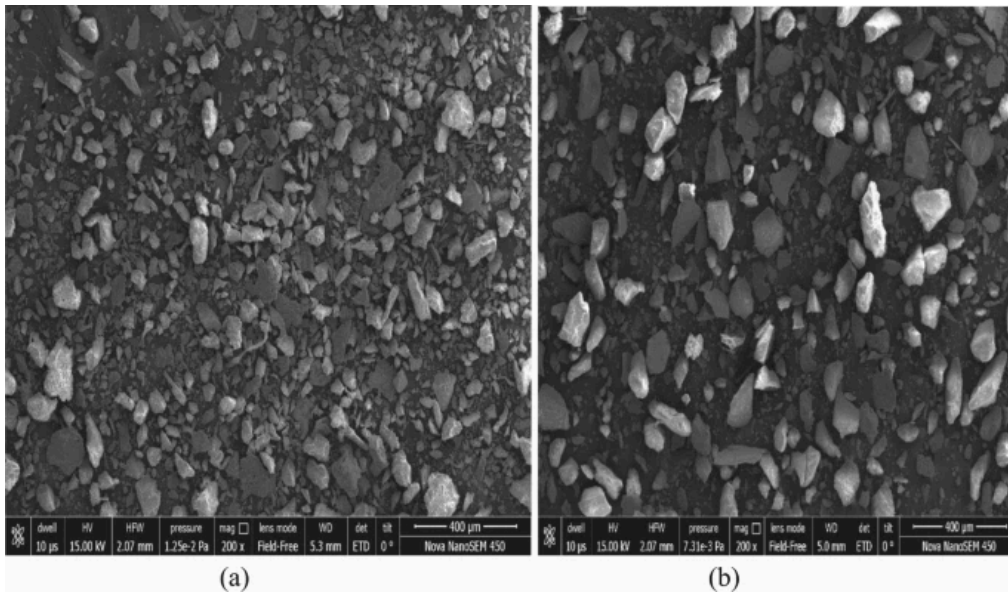
Ordinary Portland cement (OPC, 43 grade) was used as a binder, affirmed by BIS 8112 (2013). CWTA, Banas river sand (i.e. natural fine aggregate), and coarse aggregate (highest 10 mm size) were used following BIS 383 (2016). Figure 1 depicts the distribution of grain size of river sand and CWTA. Figure 2 shows that river sand particles are granular and smooth, whereas CWTA particles are rough and angular. Polycarboxylic ether Glenium Sky 877 was taken as a high water-decreasing superplasticizer. Material properties of coarse aggregates, CWTA, cement, and natural river sand are depicted in Table 1. X-ray fluorescence technique was used to assess the chemical composition of river sand and CWTA, as reported in Table 2. XRD investigation (Fig. 3) of river sand and CWTA shows the majority of quartz, albite, and microcline in river sand, whereas quartz, calcium oxide, magnesium silicate, and aluminium in CWTA.

Fig. 1



Gradation of river sand and CWTA

Fig. 2

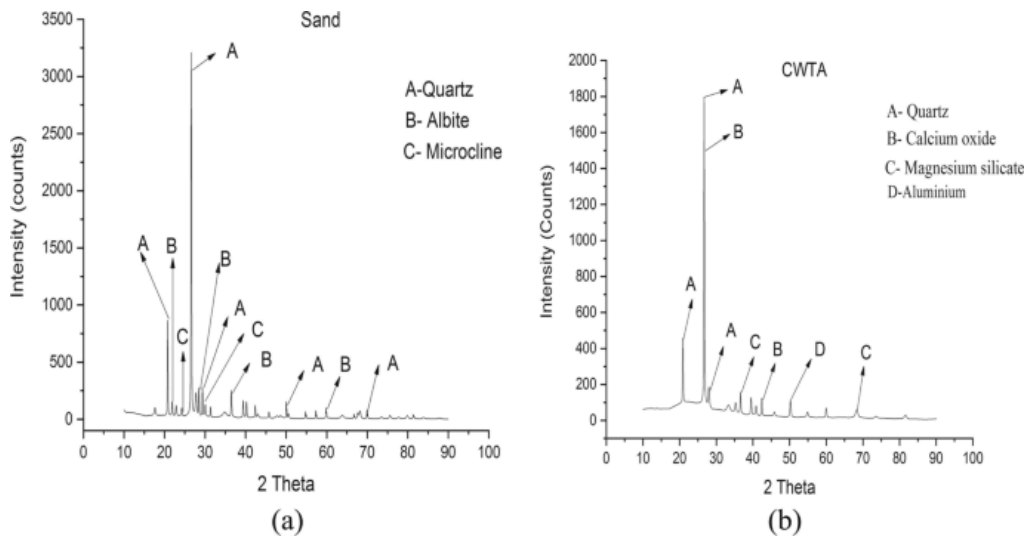


SEM images a CWTA b River sand

Table 1 Physical properties of raw materials (Vilas et al. 2022a)

Table 2 Chemical constituent of river sand and CWTA (Vilas et al. 2022a)

Fig. 3



XRD patterns a River sand b CWTA

### 3.2 Mix Proportioning

The SCC mixes (Table 3) were prepared with cement ( $560 \text{ kg/m}^3$ ) as binder material. Fine aggregate ( $928 \text{ kg/m}^3$ ) was substituted in amounts of 0, 20, 40, 60, 80 and 100% with CWTA. The total coarse aggregate quantity taken was  $731 \text{ kg/m}^3$ . A uniform w/c ratio (0.33) was selected for all mixtures. The superplasticizer amount (0.9–2.12%) was used by the weight of cement in the SCC mixture. The following nomenclature was used for SCC mixes as  $D_x$ , where x indicates the percentage substitute of CWTA with fine aggregate. Fresh characteristics were evaluated as per the requirements of EFNARC standards (EFNARC 2005). All the developed mixtures fulfilled the limitation for SCC fresh characteristics, as reported in an earlier study (Vilas et al. 2022a).

**Table 3 Self-compacting concrete mixtures ( $\text{kg/m}^3$ )**

### 3.3 Testing Procedure

#### 3.3.1 Compressive Strength

Compressive strength test was performed on 100 mm cube size specimens using a digital Compression Testing Machine (CTM) at up to 365 days of curing as per BIS 516 (1959). For assessing the compressive strength of SCC for every mix, an average of three cube specimens was taken.

#### 3.3.2 Static Modulus of Elasticity (SME)

SME was evaluated for 300 mm high and 150 mm diameter cylindrical samples, as per the standard of ASTM C469 (2002). An automatic 300-tonne CTM was used to determine SME.

#### 3.3.3 Dynamic Modulus of Elasticity (DME)

DME is a non-destructive experiment. For this experiment, 100 mm size cubic samples were used. Ultrasonic pulse velocity values and sample unit weight were determined for the assessment. DME values were calculated as per the following equation (Eq. (1)) given by Jain et al. (2020b).

$$DME = \rho V^2 / 100g \quad (1)$$

(1)

where DME in GPa,  $\rho$  = unit weight of concrete ( $\text{kg/m}^3$ ),  $g$  = gravitational acceleration equivalent to  $9.81 \text{ m/s}^2$  and  $V$  = ultrasonic pulse velocity values in (m/s).

#### 3.3.4 Chloride Penetration

This test was done on 28 days water cured cubes. Three 100 mm cubes for every SCC mixture were chosen for measuring chloride penetration, as per ASTM C1543 (2014). Samples were immersed in a 3% sodium chloride (NaCl) solution for 7, 28, 90 and 180 days. After every sample's immersion period, it was removed and surface dried with a dry fabric. The sample was then broken into two pieces, and the inner surface of it was sprayed over with 0.1 N  $\text{AgNO}_3$  solution. The free chlorine on the surface reacts with the  $\text{AgNO}_3$  and precipitates a silver-white colour of the silver chloride ( $\text{AgCl}$ ) layer, showing the penetration level of chloride.

Figure 4 displays measurements of the depth of chloride ingress in the split specimens. The average of three samples was taken as the final penetration value.

**Fig. 4**



Measurement depth of chloride ingress of SCC samples

### 3.3.5 Sulphate Attack

This experiment was conducted on 28 days water cured cubes of 100 mm in accordance with ASTM C1012 (2015). Cubes were immersed in 3% magnesium sulphate ( $\text{MgSO}_4$ ) solution for up to 180 days (Fig. 5). Magnesium sulphate solution was replenished frequently to maintain uniform concentration throughout the investigation. The impact of  $\text{MgSO}_4$  attack was measured by detecting changes in weight and compressive strength of SCC specimens as per Eqs. (2) and (3):

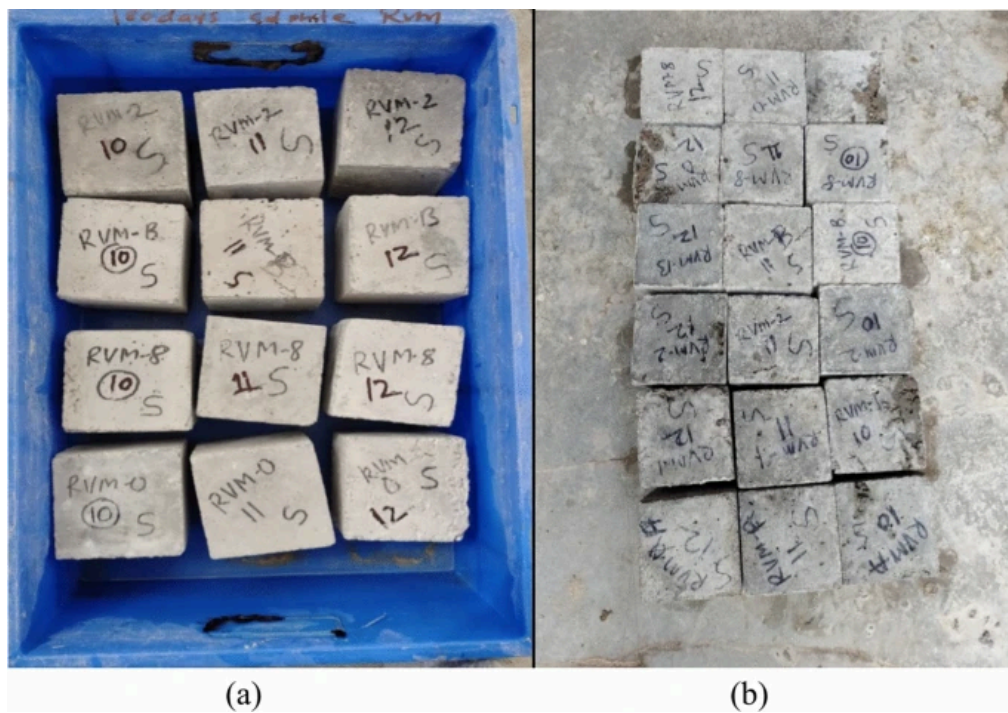
$$\text{\$ \$ } \{ \text{Variation in weight ( \% ) } \} = \frac{W_{\{a\}} - W_{\{sb\}}}{W_{\{a\}}} \times 100 \text{\$ \$}$$

(2)

$$\text{\$ \$ } \{ \text{Variation in compressive strength ( \% ) } \} = \frac{F_{\{c\}} - F_{\{sb\}}}{F_{\{c\}}} \times 100 \text{\$ \$}$$

(3)

**Fig. 5**



SCC specimens exposed to  $MgSO_4$  solution a 0 days b 180 days

Here,  $W_a$  and  $F_c$  are the oven dry weight and compressive strength of 28 days cured SCC specimen, respectively.

$W_{sb}$  and  $F_{sb}$  are the weight and compressive strength of sulphate-exposed SCC specimens on a specific day of testing, respectively.

### 3.3.6 Corrosion

Corrosion evaluation of SCC samples was performed using half-cell potential and Macro-cell current following ASTM C876 (2015) and ASTM G109 (2011), respectively. For corrosion assessments, three samples of dimensions 275 mm × 225 mm × 115 mm were prepared with ponding provision. The ponding of the sample was filled with 3% NaCl solution for 15 days, as shown in Fig. 6. Three Fe415 grade of 12 mm diameter reinforcement bars were used. One reinforcement bar 25 mm from the top and two 25 mm from the bottom were longitudinally placed before casting in the corrosion mould.

Fig. 6





Corrosion specimens with ponding facility

### 3.3.7 Carbonation

The carbonation experiment was performed on 28-day cured specimen of 50 mm × 50 mm × 100 mm size as per RILEM guidelines (Rilem and Matt [1988](#)). 50 mm × 50 mm surface of the samples was epoxy coated and then put in a carbonation chamber for 7, 14, 28, 90, 180, 365 days. The chamber was kept at a 5% CO<sub>2</sub> concentration, a 25 ± 3 °C temperature, and 50 ± 3% relative humidity. Samples were split into two halves along their length after the required exposure duration. To measure the carbonation depth, 1% phenolphthalein indicator was sprayed on split sides of the samples. Non-carbonated area changed to a pink colour, while the carbonation depth was noted in the colourless area. The mean value of three samples was recorded.

### 3.3.8 Microstructural Properties

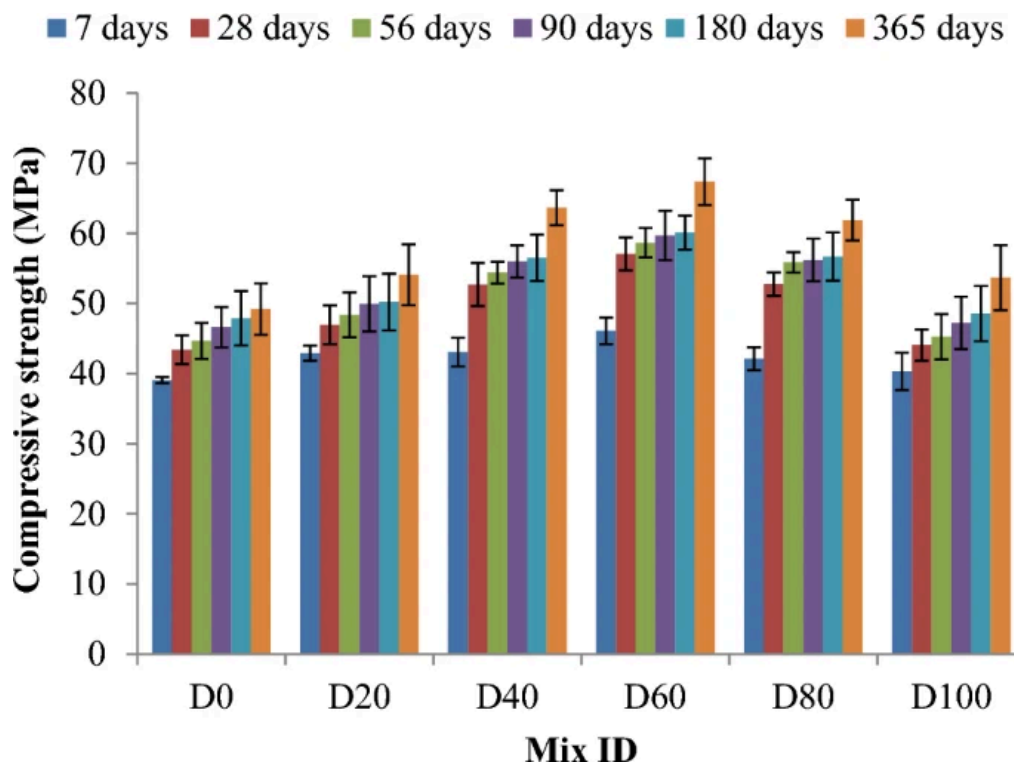
The surface morphology, void patterns, ITZ, and particle structure of SCC mixtures were examined using SEM analysis at 90 days on 10 mm cubic samples. Samples were sufficiently ground to counteract the effects of damage during cutting. Cubes were then put in the oven at 60 °C for 24 h to prevent the issue of vacuum generation. The elemental composition of the SEM samples was also observed using EDS analysis. Calcium (Ca) to silicon (Si) ratio is examined, which is often accountable for the strength of concrete composite (Choudhary et al. [2021b](#)). FTIR study using the K–Br method was done on MgSO<sub>4</sub> exposed specimens for 180 days. A powder sample was used for the FTIR study. In this analysis, wavelengths ranged between 4000 and 400 cm<sup>-1</sup>.

## 4 Results and Discussion

### 4.1 Compressive Strength

The observations of the compressive strength experiment showed that substitution of fine aggregate with CWTA in SCC increased strength at all ages ranging from 7 to 365 days (Fig. 7). The highest and lowest compressive strength values were found at 60% replacement and for control mix, respectively.

Fig. 7



Influence of CWTA on compressive strength of SCC

The 28 days compressive strength of the control mix improved from 43.42 to 57.05 MPa for 60% CWTA substitution. Similarly, 365 days compressive strength improved from 49.20 MPa to 67.35 MPa for 60% CWTA substitution. This increment might be possible due to the pozzolanic nature of CWTA, which produced a denser matrix (as observed by SEM analysis in Sect. 4.8.1). The enhanced strength might be due to the pore refinement of the resulting concrete, which was related to the smaller size of CWTA particles compared to fine aggregate. The rough surface and irregular shape of CWTA might also be the reason for better interlocking between aggregate and cement paste, in turn improving the compressive strength of the mix. However, incorporating CWTA beyond an optimum level (greater than 60% GP in the present case) slashed the filler effect. Hence, the increase in inter-particle voids for incorporating CWTA of more than 60% initiated the reduction of compressive strength.

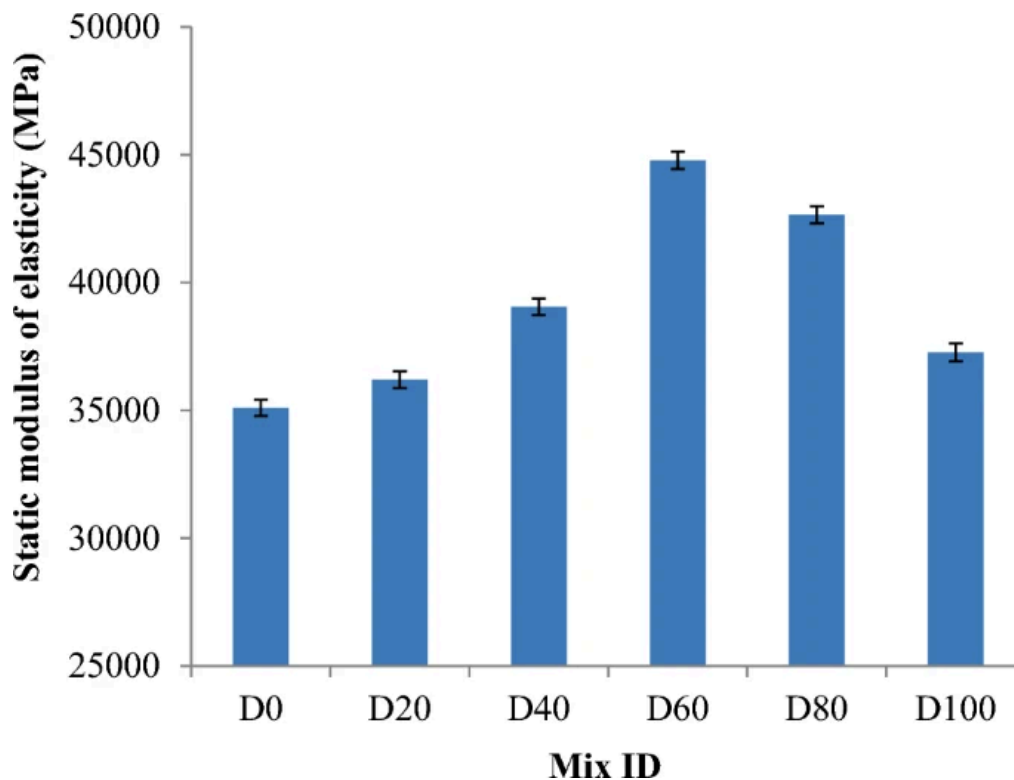
Earlier researchers observed similar variations in the compressive strength for CWTA-modified concrete. Faldessai et al. (2023) detected enhanced compressive strength on 25% cement substitution with waste ceramic. Gautam et al. (2022a) observed enhanced strength on 10% cement substitution with waste bone china ceramic. Medina et al. (2012b) found higher strength for substituting up to 25% coarse aggregate with waste sanitary ceramic. Rashid et al. (2017) also revealed an augmentation in compressive strength for concrete blends incorporating up to 30% waste ceramic as a coarse aggregate. Other studies have also

mentioned increased compressive strength using ceramic waste (Awoyera et al. [2018](#); Bommisetty et al. [2019](#); Guerra et al. [2009](#); Keshavarz and Mostofinejad [2019](#)).

## 4.2 Static Modulus of Elasticity (SME)

Figure 8 depicts the SME observed for different SCC mixtures at 28 days of curing. The trend of rising SME with the increase in CWTA content is similar to the trend for compressive strength. For the substitution of 60% CWTA (D<sub>60</sub> mix), SCC recorded the maximum SME. The roughness of the CWTA increased the interlocking between cement paste and aggregate (Siddique et al. [2018c](#)), thereby causing an increase in SME. It may also be noted that the prominent factors affecting the SME are the stiffness of mortar paste and coarse aggregate, the porosity, and the bond of paste with aggregate (Rashid et al. [2017](#)). The stiffness of the paste increased on substituting river sand with CWTA due to its better packing effect, thereby causing an improved SME.

Fig. 8



Influence of CWTA on SME of SCC

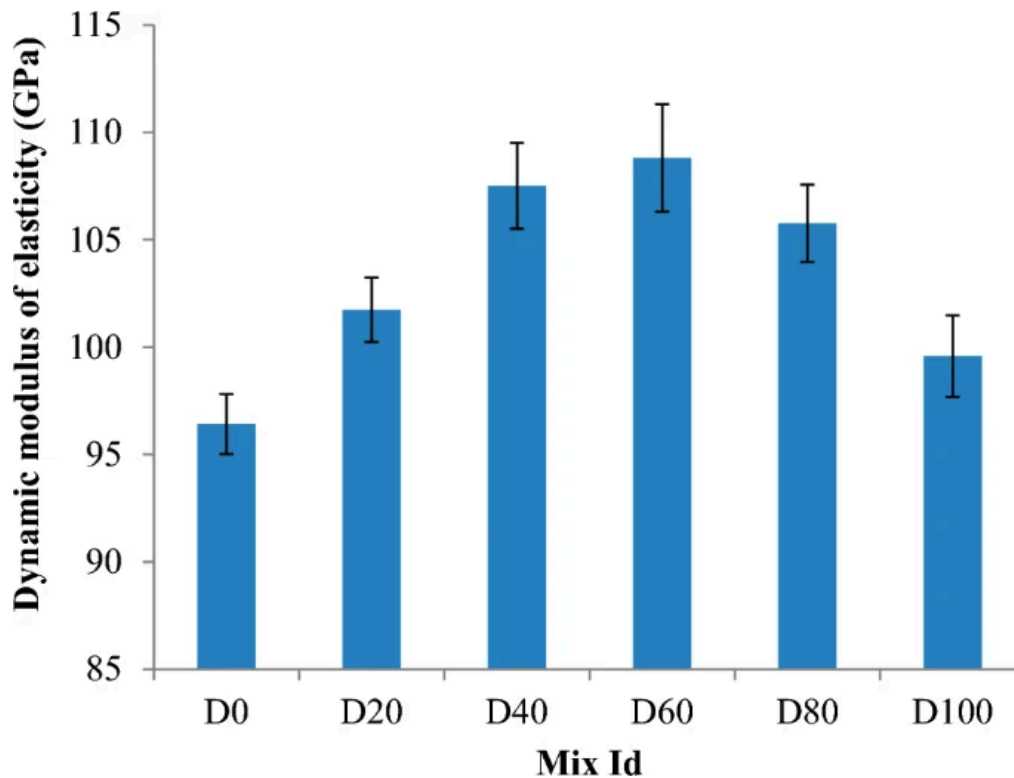
Anderson et al. ([2016](#)) found an increase in SME on substituting up to 100% coarse aggregate with waste ceramic aggregate. Similarly, Siddique et al. ([2018c](#)) also stated an increment in SME on incorporating up to 100% waste ceramic fine aggregate in vibrated concrete.

## 4.3 Dynamic Modulus of Elasticity (DME)

DME results for 28-day cured SCC specimens are displayed in Fig. 9. This experiment was conducted by measuring ultra-pulse velocity without applying stress (Vilas et al. [2022a](#)). CWTA inclusion in the SCC

mixture resulted in an increment in DME. The outcome established that all CWTA-based SCC mixes have more DME than  $D_0$  mix. Maximum DME was found for  $D_{60}$  mix compared to  $D_0$  mix.

Fig. 9



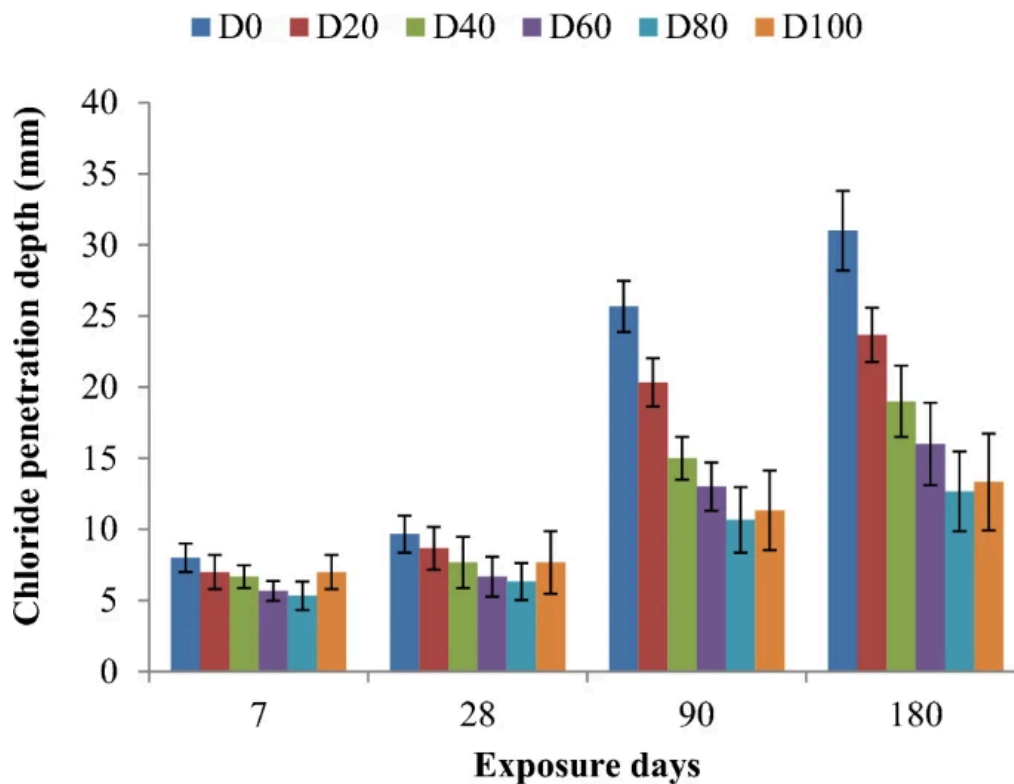
Influence of CWTA on DME of SCC mixtures

This behaviour could be credited to lower voids and water absorption of CWTA-based SCC mixes associated with the finer particles of CWTA than fine aggregate (Vilas et al. [2022a](#)). In addition, higher formation of CSH gel in CWTA-based mixes led to strong interfacial transition zones, which might have influenced modulus of elasticity. A similar experiment result was also observed by Anderson et al. ([2016](#)), who stated the increment in modulus of elasticity by 26.9% for concrete prepared with up to 100% ceramic tile waste.

#### 4.4 Chloride Penetration

It can be witnessed from Fig. [10](#) that chloride penetration depth reduced with the rise in CWTA content. The minimum chloride penetration depth was witnessed for  $D_{80}$  mix at all immersion period. However, the highest chloride penetration depth was found for  $D_0$  mix. This improved resistance against chloride penetration was attributed to the rough surface and pozzolanic nature of CWTA (Siddique et al. [2018a](#)). The dense and pore microstructure refinement enhanced resistance against chloride penetration, owing to the incorporation of finer CWTA particles. The formation of the tortuous path within the CWTA-based SCC might also decrease the chloride penetration due to the angular shape of CWTA (Jain et al. [2022b](#)). Siddique et al. ([2019](#)) detected decreased chloride penetration depth values for entirely substituting river sand with bone china ceramic in concrete. Ali et al. ([2016](#)) also concluded a reduction in chloride ions permeability with the incorporation of waste ceramic powder in concrete.

Fig. 10



Influence of CWTA on chloride penetration depth of SCC mixes

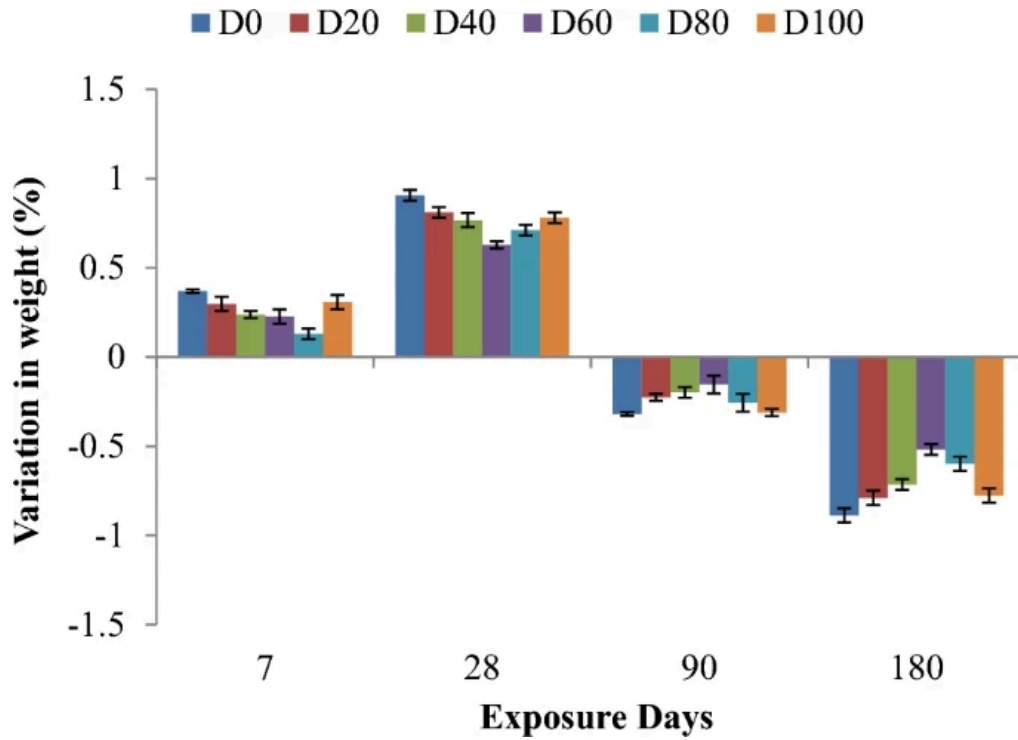
## 4.5 Sulphate Attack

Sewerage water, groundwater and  $\text{Ca}(\text{OH})_2$  are leading causes of sulphate attack in concrete. Chemical action between sulphate and  $\text{Ca}(\text{OH})_2$  generates byproducts like thaumasite, expansive ettringite and gypsum, which are often root causes of concrete deterioration (Neville [2004](#)). To simulate the sulphate attack on concrete,  $\text{MgSO}_4$  solution was used.

### 4.5.1 Change in Weight

Figure [11](#) depicts weight change in the SCC samples immersed in  $\text{MgSO}_4$  solution. It was found that weight increased continuously up to 28 days exposure for all SCC mixtures. This might be owing to the development of gypsum and ettringite within voids of SCC samples. However, at ages 90 and 180 days, weight loss was observed. During the later stages of test,  $\text{MgSO}_4$  causes a significant damaging impact on hydration products due to the expansive nature of gypsum and ettringite. Weight loss was also observed due to the decay of CSH gel in reaction with  $\text{MgSO}_4$  (Nyunin [1984](#)). Nevertheless, concrete mixes containing CWTA have shown lower weight loss than  $\text{D}_0$  mix. After 180 days, mix  $\text{D}_{60}$  performed superior to all other SCC mixes. The lower weight loss of CWTA-based SCC mixes after exposure to sulphate attack might be due to the low decay of portlandite and CSH gel than  $\text{D}_0$  mix (as observed in FTIR analysis Sect. [4.8.3](#)). Earlier, Siddique et al. ([2018b](#)) also observed lower weight loss for concrete containing ceramic aggregate after exposure to sulphate attack. Gautam et al. ([2023](#)) observed lower weight loss for granite-based SCC containing bone-china ceramic powder as a substitute to cement.

Fig. 11

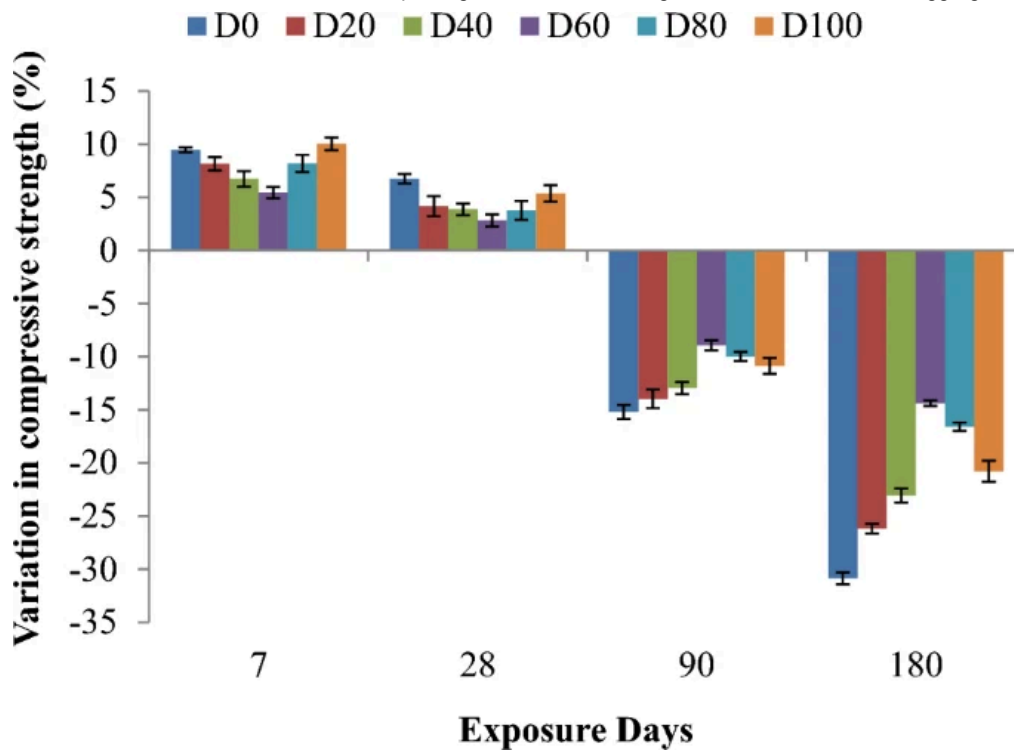


Variation in weight of CWTA-based SCC after exposure to sulphate attack

#### 4.5.2 Change in Compressive Strength

The changes in compressive strength for 7, 28, 90 and 180 days exposure to  $MgSO_4$  are depicted in Fig. 12. Maximum decrement in compressive strength percentage was found for  $D_0$  mix. However, maximum residual strength was noticed for  $D_{60}$  mixture at all ages, showing better performance of SCC containing CWTA against sulphate attack.

Fig. 12



Variation in compressive strength of CWTA-based SCC after exposure to sulphate attack

These outcomes are in correlation with the variation in weight. The enhancement in sulphate attack resistance of CWTA-based SCC can be attributed to the robust nature of CWTA, which is less reactive when it comes into contact with the  $MgSO_4$  solution. The refined microstructure and tortuous path in CWTA-based SCC prevent the ingress of sulphate ions due to the finer and angular shape CWTA particles. Outcomes analogous to these were also stated by Siddique et al. (2018b), who substituted waste ceramic bone china with fine aggregate. Mixtures with 100% bone china fine ceramic aggregate noted the minimum loss in compressive strength percentage after exposure to 180 days. Cheng et al. (2014) stated that replacing up to 40% cement with ceramic polishing powder in concrete slightly enhanced the sulphate resistance properties.

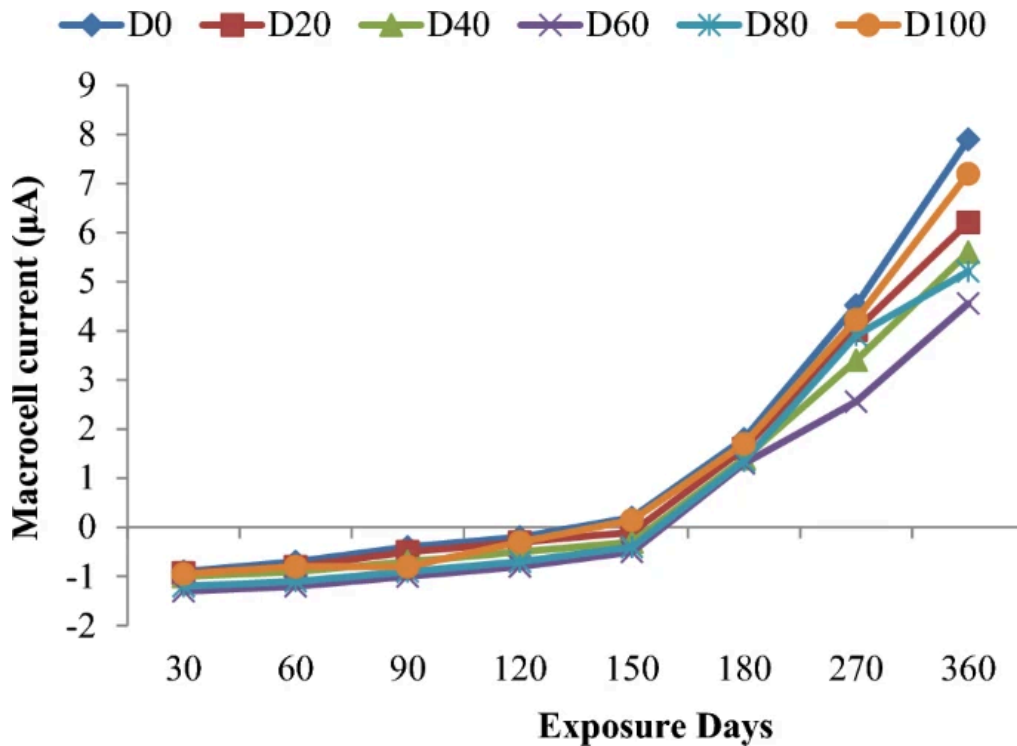
## 4.6 Corrosion Test

Chloride solution was used to measure corrosion resistance of SCC mixes. Free chloride ions often start corrosion of steel bars present in concrete. The corrosion experiment data are organized into expressions focusing on macro-cell current and the potential values measured at half-cells. This classification helps us better understand and interpret the corrosion behaviour of the material under investigation.

### 4.6.1 Macrocell Current

Figure 13 depicts the results of macrocell current found for CWTA-based SCC. Macrocell current values for all mixes were observed to be less than  $+10\mu A$  for the whole analysis duration, which indicated zero corrosion possibility. It can also be observed that corrosion for all mixes did not initiate even after 360 days of testing. The values found for CWTA-based SCC showed an increment in resistance against corrosion than  $D_0$  mix. The increased resistance against corrosion for CWTA-based SCC is owing to microstructure densification associated with the filler efficacy of CWTA. The additional formation of CSH gel in CWTA-based mixes works as a block by absorbing the chloride ions (Siddique et al. 2019), thereby causing an increment in resistance against corrosion.

Fig. 13



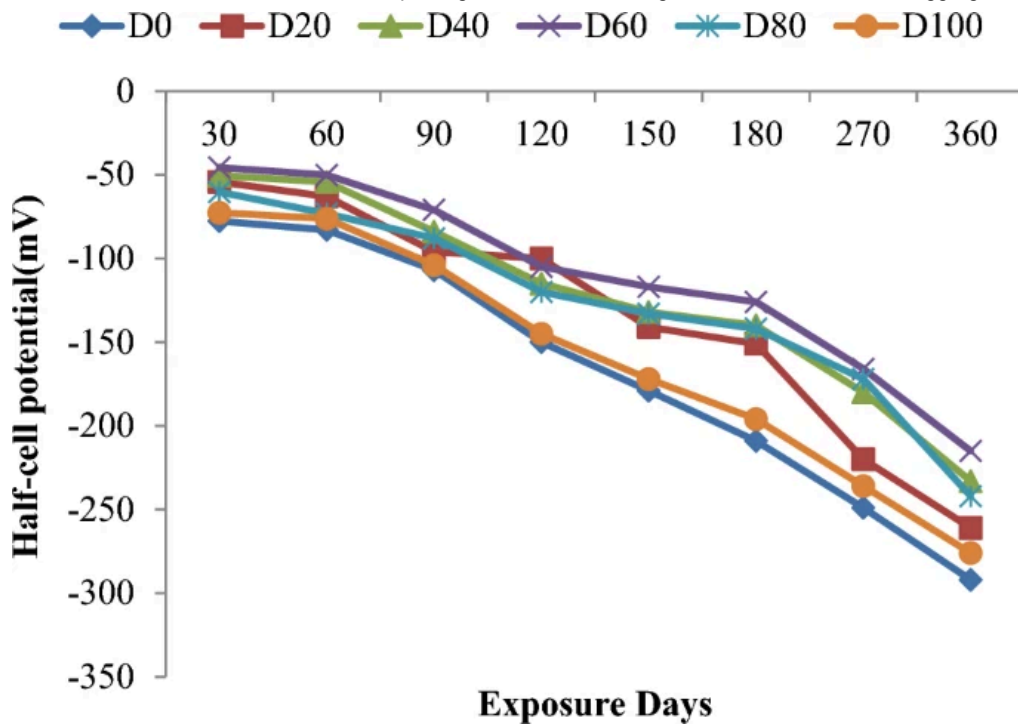
Macrocell current of SCC mixes

#### 4.6.2 Half-Cell Potential

Figure 14 depicts results of half-cell potential (consistent with outcomes of macro-cell current) for CWTA-based SCC. Half-cell potential values varying from 0 to  $-200$  mV,  $-200$  to  $-350$  mV, and more than  $-350$  mV depict a 90% possibility of zero corrosion, unclear corrosion, and 90% possibility of corrosion, respectively. A weak concrete microstructure, along with higher voids, generally creates samples highly prone to corrosion. However, CWTA-based SCC with relatively better microstructure depicts greater corrosion resistance than  $D_0$  mix. Another reason could be the angular and rough particles of CWTA, which form the tortuous path within the concrete, thereby limiting the ingress of chloride ions. The outcomes were consistent with the results revealed by Siddique et al. (2019). Jeronimo et al. (2018) observed a decrease in the chloride transport rate of concrete on 20%–30% substitution of cement with waste ground clay bricks.

Fig. 14



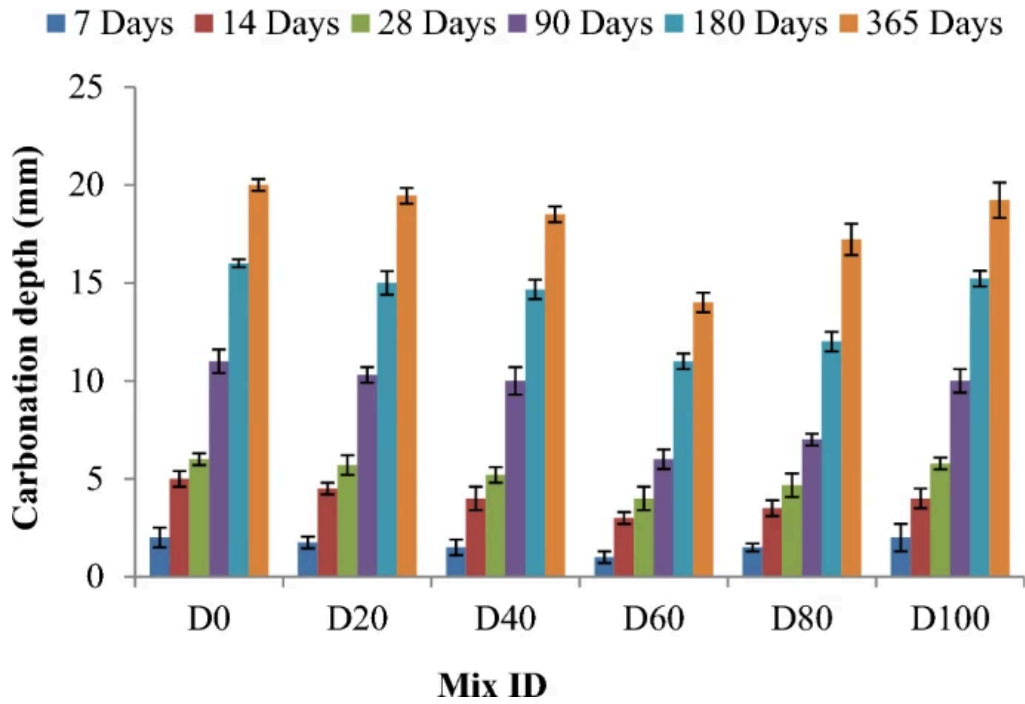


Half-cell potential of SCC mixes

#### 4.7 Carbonation test

The experimental results of the carbonation experiment up to 365 days of exposure are displayed in Fig. 15. Mix containing up to 60% CWTA had minimum carbonation depth compared to D<sub>0</sub> mix. Moreover, all other CWTA-based SCC showed lower carbonation depth than D<sub>0</sub> mix. The lower carbonation depth for CWTA-based SCC mixes might be due to the better pore packing efficacy of CWTA. The decrement of permeable voids on the inclusion of CWTA might also result in lower carbonation depth (Vilas et al. 2022a). The roughness in texture of CWTA reduces the continuity of capillary paths, which leads to better carbonation resistance for SCC containing CWTA. The development of strong microstructure on incorporation of CWTA also increased the carbonation resistance (Vilas et al. 2022a). Earlier, Medina et al. (2012a) also discerned an improvement in carbonation resistance by including recycled ceramic aggregate in concrete. The minimal cover provided for the reinforcement for moderate and mild exposure levels is 30 mm and 20 mm as per BIS 456 (2000), respectively, which is more than 20 mm (the maximum value for carbonation depth). The carbon dioxide content in the environment is around 0.04%, but a 5% level was maintained in the carbonation chamber, which is 125 times greater than atmosphere level (Esquinas et al. 2018). Therefore, all mixtures could be regarded as harmless against carbonation-related corrosion.

Fig. 15



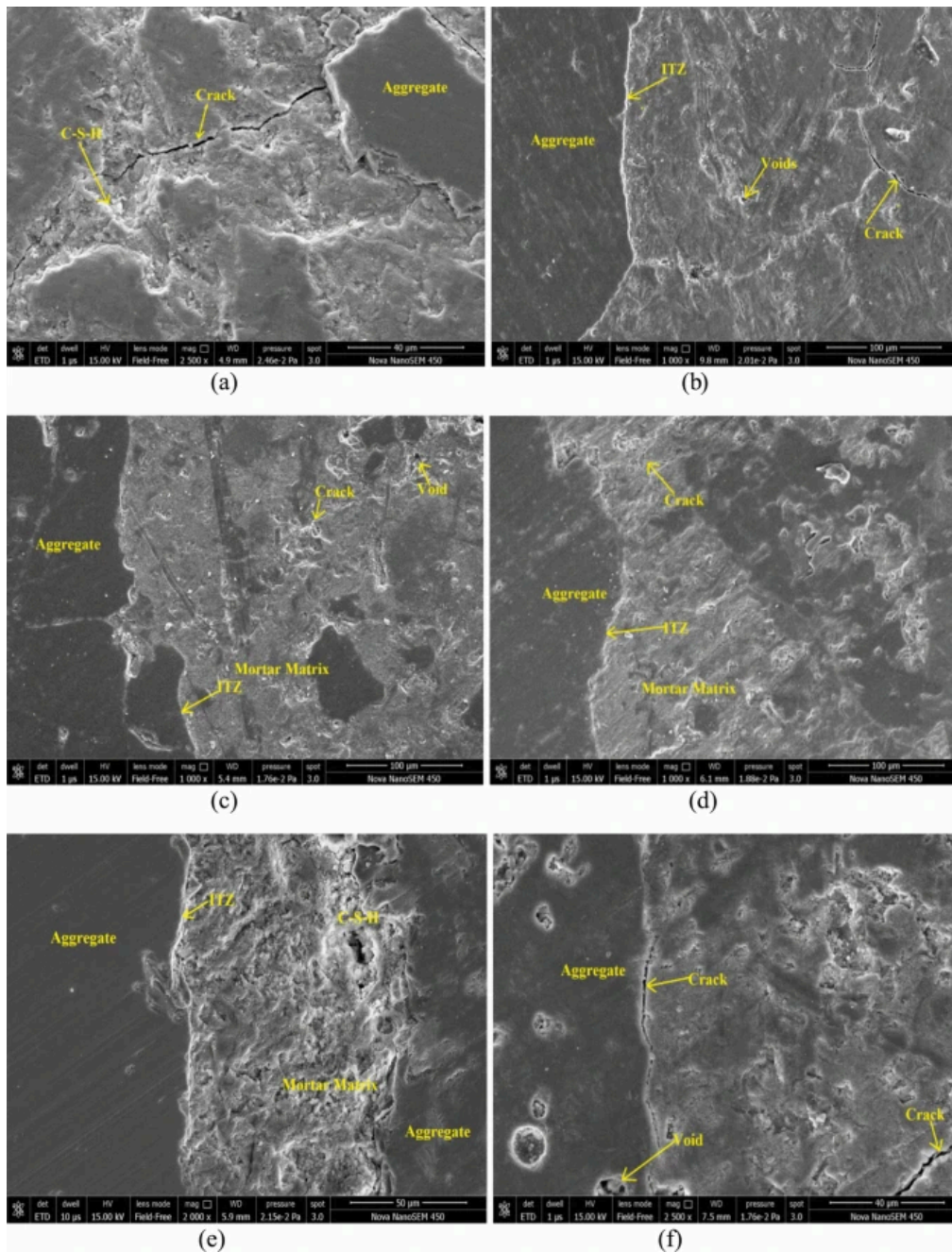
Influence of CWTA on carbonation depth of SCC mixtures

## 4.8 Microstructural Properties

### 4.8.1 SEM Analysis

Figure 16 shows SEM micrographs of all SCC mixtures (a–f). The presence of voids, cracks, CSH gel, and interfacial transition zone (ITZ) were seen in the SEM micrograph.

Fig. 16



Microstructure images of all SCC mixtures a  $D_0$ ; b  $D_{20}$ ; c  $D_{40}$ ; d  $D_{60}$ ; e  $D_{80}$ ; f  $D_{100}$

In the control and  $D_{100}$  mixes, there are evident surface fissures and poor ITZ. An SCC mix with 60% CWTA showed reduced crack width and enhanced ITZ relative to the control mix, which might cause enhanced mechanical performance. The compacted and dense microstructure for  $D_{60}$  (Fig. 16d) mix owing to the better distribution of CSH gel (Gautam et al. 2022c). Incorporating CWTA in SCC mixtures resulted in enhanced ITZ and no discernible crack. Siddique et al. (2017) also reported similar results for concrete mixes. It can be concluded that a 60% CWTA was the optimum substitution, where CWTA considerably filled the pores of SCC.

#### 4.8.2 EDS Analysis

The elemental compositions along with Ca/Si (calcium to silica) ratio were examined, which demonstrates the C–S–H gel formation in the SCC mix (Gupta and Siddique 2020; Jain et al. 2020a). The other elements observed by EDS analysis are Fe, Al, Mg, C, Na, K, O, and Ti. Reduction in Ca/Si ratio suggests the CSH gel formation, thus improving the compressive strength of SCC. It is clear from Table 4 that  $D_{60}$  has the lowest

Ca/Si ratio when related to other mixtures with varying proportions of CWTA. Maximum silica content was observed in 60% CWTA-based SCC mixture. It can be stated that an increase in the amount of silica develops a better pozzolanic reaction. The formation of the CSH gel might be responsible for the increased strength and durability characteristics of CWTA-based SCC.

---

#### Table 4 Elemental composition of SCC mixes

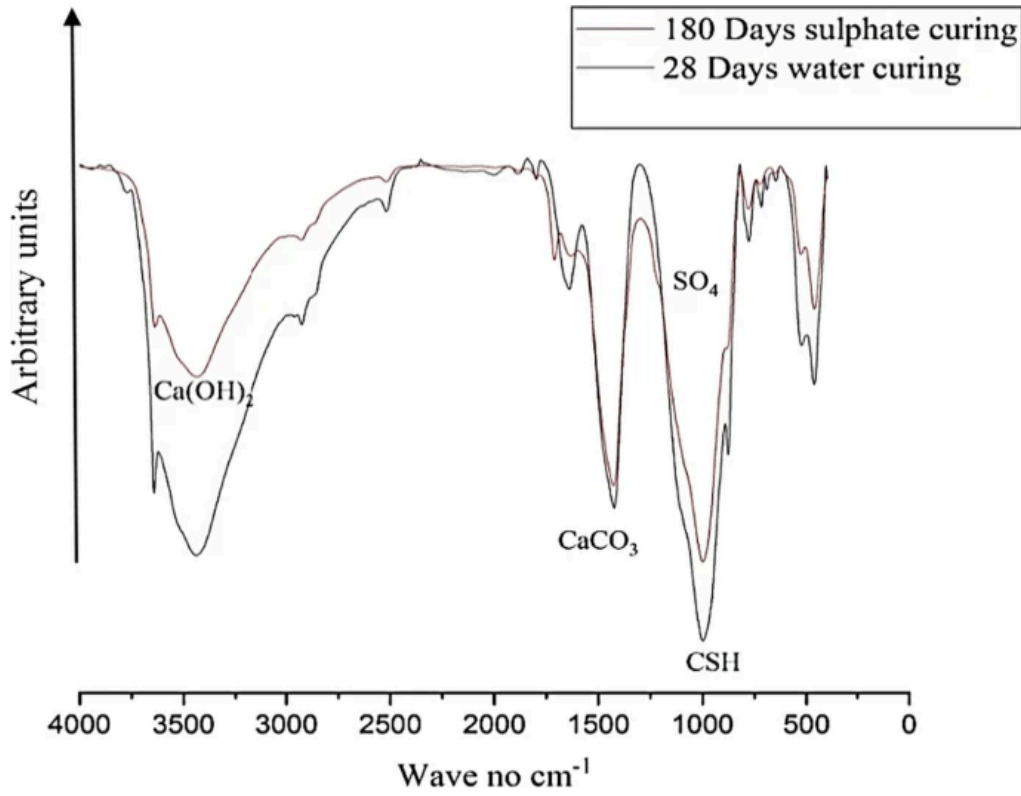
---

#### 4.8.3 Sulphate Attack FTIR Analysis

Figures [17](#), [18](#), [19](#), [20](#), [21](#), and Fig. [22](#) display the FTIR results for 28 days water cured and 180 days sulphate-exposed samples. As shown in Table [5](#), substantial change is seen in molecular groups of Si–O (CSH gel), O–H ( $\text{Ca}(\text{OH})_2$  or portlandite) and  $\text{SO}_4$  (ettringite). Bands of ettringite, CSH gel and  $\text{Ca}(\text{OH})_2$  are observed around  $1109\text{--}1131\text{ cm}^{-1}$  (Bisht and Ramana [2019](#)),  $968\text{--}1006\text{ cm}^{-1}$  (Rubio et al. [1997](#); Siddique et al. [2021](#)) and  $3614\text{--}3645\text{ cm}^{-1}$  (Guo et al. [2019](#); Številca et al. [1994](#)), respectively. Sulphate-exposed specimens showed lower wave number for portlandite bands when related to water cured specimens. The development of additional peaks of ettringite bands was also observed for sulphate exposed specimens. The consumption of  $\text{Ca}(\text{OH})_2$  and the development of ettringite groups indicate sulphate attack. It may also be noted that the moving of bands to lower wave numbers shows its weakening (Bisht and Ramana [2019](#); Siddique et al. [2018b](#)). Sulphate-exposed SCC mixes containing CWTA showed lower shifting of portlandite bands than control mix, inferring greater sulphate attack resistance by CWTA-based SCC mixes. The CSH gel bands were also moved to lower side for all the mixes when exposed to sulphate solution. However, CWTA-based SCC mixes showed a lower drop in CSH gel bands than  $D_0$  mix on exposure to sulphate, demonstrating higher sulphate resistance of CWTA-based SCC mixes. The lower decay of portlandite and CSH gel for CWTA-based SCC mixes might be the prime cause for their higher strength against sulphate attack.

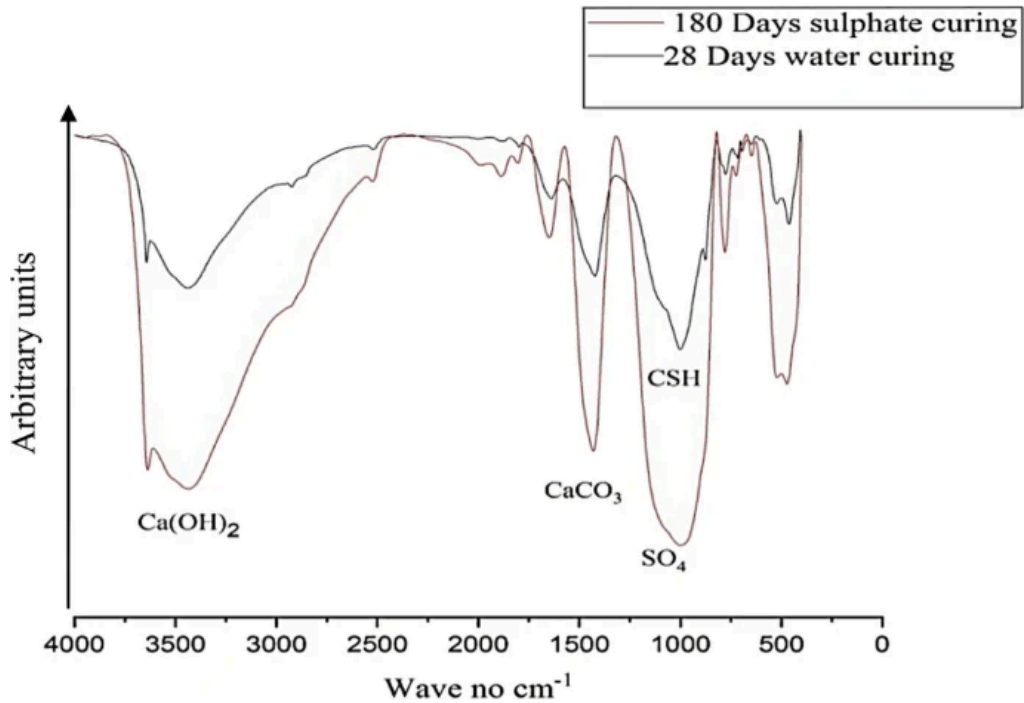
---

#### Fig. 17



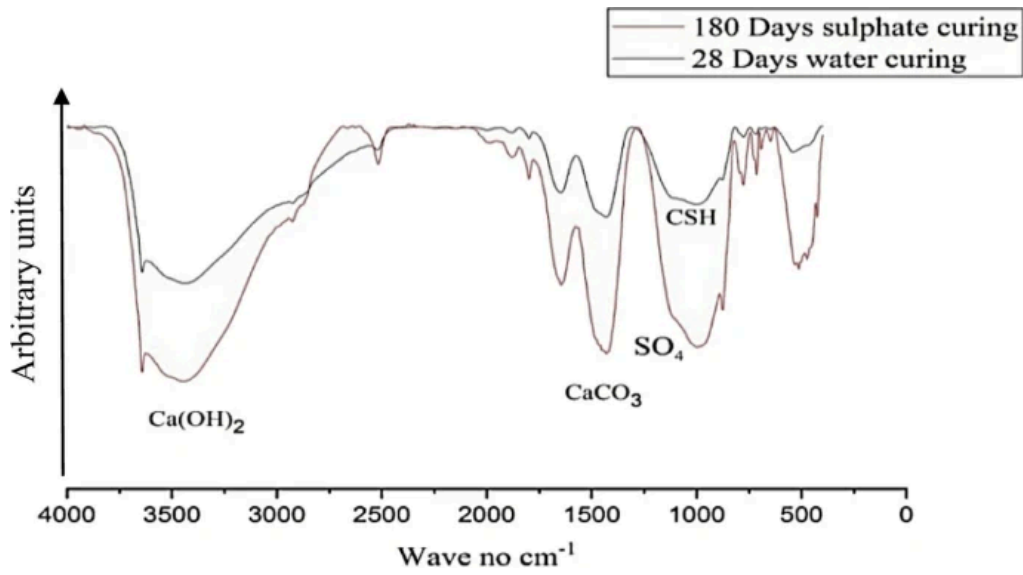
FTIR spectra for  $D_0$  mix at 180 days  $\text{MgSO}_4$  exposure period

Fig. 18



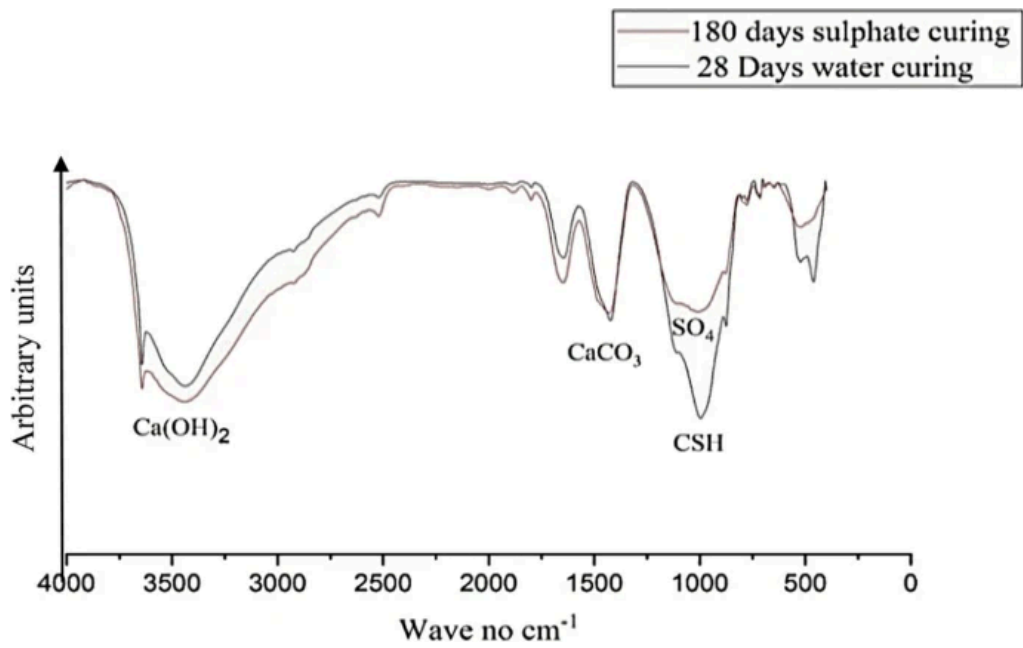
FTIR spectra for  $D_{20}$  mix at 180 days  $\text{MgSO}_4$  exposure period

Fig. 19



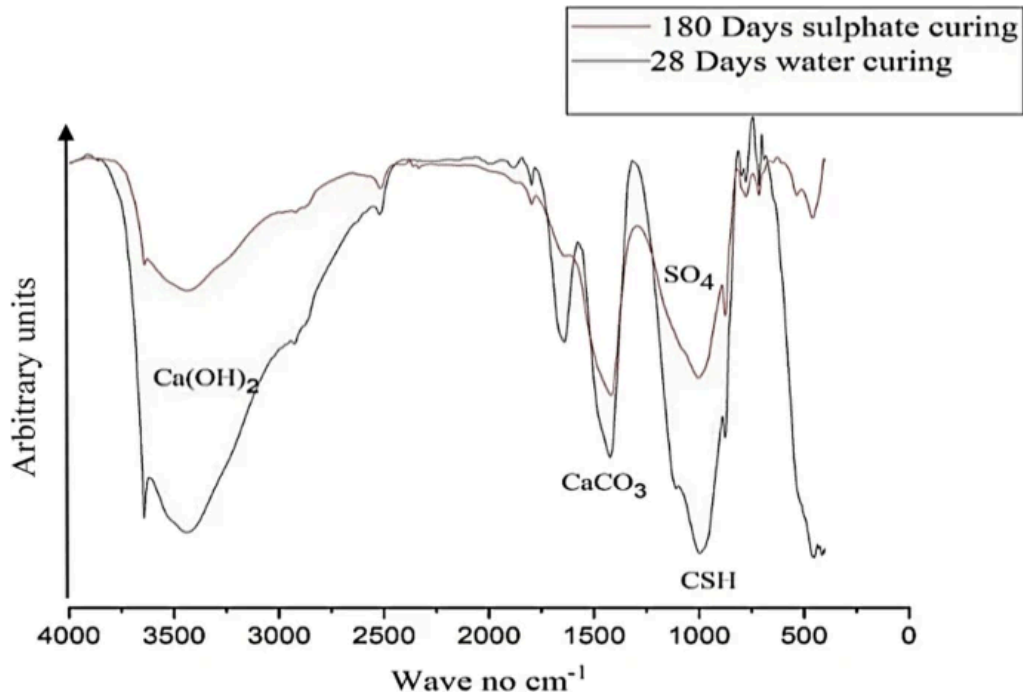
FTIR spectra for  $D_{40}$  mix at 180 days  $\text{MgSO}_4$  exposure period

Fig. 20



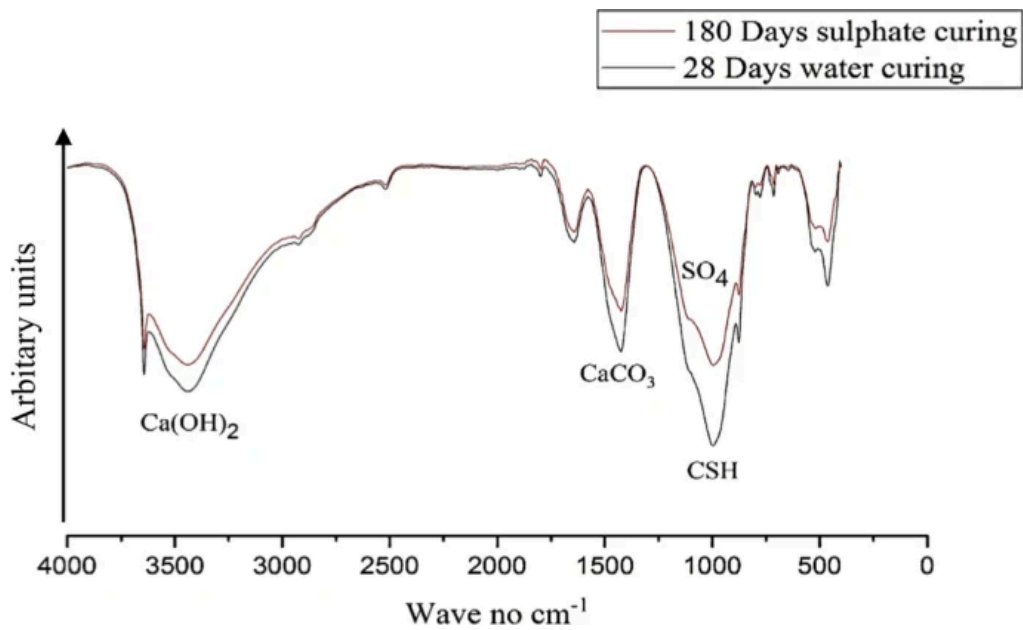
FTIR spectra for  $D_{60}$  mix at 180 days  $\text{MgSO}_4$  exposure period

Fig. 21



FTIR spectra for D<sub>80</sub> mix at 180 days MgSO<sub>4</sub> exposure period

Fig. 22



FTIR spectra for D<sub>100</sub> mix at 180 days MgSO<sub>4</sub> exposure period

Table 5 FT-IR wave numbers (cm<sup>-1</sup>) examined on CWTA self-compacting concrete samples

## 5 Conclusions

This study promotes the use of CWTA in place of natural fine aggregate in the manufacturing of SCC. The following conclusions can be drawn on completing the experimental work.

- Compressive strength was increased for SCC mixes containing up to 60% CWTA than reference SCC.
- An increment in modulus of elasticity was observed for SCC mixes containing up to 100% CWTA relative to the control mix.
- CWTA-based SCC showed superior resistance to chloride penetration and carbonation than the reference SCC. Moreover, the lowest penetration depth was found for the optimum mix (i.e. D<sub>60</sub> mix).
- Slight alterations have been noticed in compressive strength and weight of CWTA-based SCC mixes on sulphate attack. The primary reason for this could be the reduced chances of disintegration of SCC constituents on sulphate attack due to the durable and less reactive behaviour of CWTA.
- The initiation of corrosion was not observed for any mix, even after an exposure of 12 months. The corrosion experiment also revealed significant resistance to corrosion for D<sub>60</sub> mix. The tortuosity and considerable CSH gel in CWTA-based SCC provided a higher resistance against corrosion.
- D<sub>60</sub> mixture showed improved microstructural properties. SEM study revealed an enhanced interfacial transition zone (ITZ) and fewer voids.
- EDS analysis revealed a decrement in Ca/Si ratio for incorporating up to 60% CWTA in SCC compared to reference SCC, causing higher strength for CWTA-based SCC matrix. The lower Ca/Si ratio also suggested the higher development of CSH gel in CWTA-based SCC.
- FTIR analysis confirmed the lower deterioration of portlandite and CSH gel in CWTA-based SCC mixes than control SCC mix on exposure to sulphate attack.

As an outcome of this research, incorporating up to 60% CWTA can be recommended as a feasible substitute to fine aggregate in SCC structures subjected to harsh environments.

## References

---

Ali ST, EL-Dieb AS, Aboubakr SH, Reda Taha MM (2016) Utilization of ceramic waste powder in self-compacting concrete. *Sustain. Constr. Mater. Technol.* 2016–August

Anderson DJ, Smith ST, Au FTK (2016) Mechanical properties of concrete utilising waste ceramic as coarse aggregate. *Constr Build Mater* 117:20–28. <https://doi.org/10.1016/j.conbuildmat.2016.04.153>

[Article](#) [Google Scholar](#)

ASTM C1012 (2015) Standard test method for length change of hydraulic-cement mortars exposed to a sulfate solution. *ASTM Int.* West Conshohocken, PA 11, 5–9. <https://doi.org/10.1520/C1012>



ASTM C1543 (2014) Standard test method for determining the penetration of chloride ion into concrete by ponding. ASTM Int. West Conshohocken, 1–4 <https://doi.org/10.1520/C1543-10a.2>

ASTM C469 (2002) Standard test method for static modulus of elasticity and Poisson's ratio of concrete in compression. ASTM Stand. B. 04, 1–5

ASTM C876 (2015) Standard test method for corrosion potentials of uncoated reinforcing steel in concrete. ASTM Int. West Conshohocken, 1–8. <https://doi.org/10.1520/C0876-15.2>

Awoyera PO, Ndambuki JM, Akinmusuru JO, Omole DO (2018) Characterization of ceramic waste aggregate concrete. HBRC J 14:282–287. <https://doi.org/10.1016/j.hbrcj.2016.11.003>

[Article](#) [Google Scholar](#)

BIS 383 (2016) Specification for coarse and fine aggregates from natural sources for concrete. Bur. Indian Stand., New Delhi, India

BIS 456 (2000) Plain concrete and reinforced concrete. Bur. Indian Stand., New Delhi, India

BIS 516 (1959) Method of tests for strength of concrete. Bur. Indian Stand., New Delhi, India

BIS 8112 (2013) ORDINARY PORTLAND CEMENT, 43 grade specification, Bur. Indian Stand., New Delhi, India

Bisht K, Ramana PV (2019) Waste to resource conversion of crumb rubber for production of sulphuric acid resistant concrete. Constr Build Mater 194:276–286. <https://doi.org/10.1016/j.conbuildmat.2018.11.040>

[Article](#) [Google Scholar](#)

Bommisetty J, Keertan TS, Ravitheja A, Mahendra K (2019) Effect of waste ceramic tiles as a partial replacement of aggregates in concrete. Mater. Today Proc 8–10. <https://doi.org/10.1016/j.matpr.2019.08.230>

Cheng Y, Huang F, Li GL, Xu L, Hou J (2014) Test research on effects of ceramic polishing powder on carbonation and sulphate-corrosion resistance of concrete. Constr Build Mater 55:440–446. <https://doi.org/10.1016/j.conbuildmat.2014.01.023>

[Article](#) [Google Scholar](#)

Choudhary R, Gupta R, Alomayri T, Jain A, Nagar R (2021a) Permeation, corrosion, and drying shrinkage assessment of self-compacting high strength concrete comprising waste marble slurry and fly ash, with

silica fume. Structures 33:971–985. <https://doi.org/10.1016/j.istruc.2021.05.008>

[Article](#) [Google Scholar](#)

Choudhary R, Gupta R, Nagar R, Jain A (2021b) Mechanical and abrasion resistance performance of silica fume, marble slurry powder, and fly ash amalgamated high strength self-consolidating concrete. Constr Build Mater 269:121282. <https://doi.org/10.1016/j.conbuildmat.2020.121282>

[Article](#) [Google Scholar](#)

Chouhan HS, Kalla P, Nagar R, Gautam PK (2019) Gainful utilization of dimensional limestone waste as fine aggregate in cement mortar mixes. Constr Build Mater 221:363–374.

<https://doi.org/10.1016/j.conbuildmat.2019.06.097>

[Article](#) [Google Scholar](#)

Concrete, Cement, Concrete, Curing, Cabinets M, Rooms M (2011) Standard test method for determining effects of chemical admixtures on corrosion of embedded steel reinforcement in concrete exposed to 07, 3–8. <https://doi.org/10.1520/G0109-07R13.2>

Dezhampanah S, Nikbin IM, Charkhtab S, Fakhimi F, Bazkiaei SM, Mohebbi R (2020) Environmental performance and durability of concrete incorporating waste tire rubber and steel fiber subjected to acid attack. J Clean Prod 268:122216. <https://doi.org/10.1016/j.jclepro.2020.122216>

[Article](#) [Google Scholar](#)

EFNARC (2005) The European guidelines for self-compacting concrete. Eur. Guidel. Self Compact. Concr. 63

Esquinas AR, Álvarez JI, Jiménez JR, Fernández JM (2018) Durability of self-compacting concrete made from non-conforming fly ash from coal-fired power plants. Constr Build Mater 189:993–1006.

<https://doi.org/10.1016/j.conbuildmat.2018.09.056>

[Article](#) [Google Scholar](#)

Faldessai K, Lawande S, Kelekar A, Gurav R, Kakodkar S (2023, nd) Utilization of ceramic waste as a partial replacement for cement in concrete manufacturing, Mater Today: Proc, ISSN 2214-7853.

<https://doi.org/10.1016/j.matpr.2023.06.453>

Gautam L, Jain JK, Jain A, Kalla P (2022a) Recycling of bone china ceramic waste as cement replacement to produce sustainable self-compacting concrete. Structures 37:364–378.

<https://doi.org/10.1016/j.istruc.2022.01.019>

[Article](#) [Google Scholar](#)

Gautam L, Kalla P, Jain JK, Choudhary R, Jain A (2022b) Robustness of self-compacting concrete incorporating bone china ceramic waste powder along with granite cutting waste for sustainable development. *J Clean Prod* 367:132969. <https://doi.org/10.1016/j.jclepro.2022.132969>

[Article](#) [Google Scholar](#)

Gautam L, Kumar Jain J, Jain A, Kalla P (2022c) Valorization of bone-china ceramic powder waste along with granite waste in self-compacting concrete. *Constr Build Mater* 315:125730. <https://doi.org/10.1016/j.conbuildmat.2021.125730>

[Article](#) [Google Scholar](#)

Gautam L, Bansal S, Sharma KV, Kalla P (2023) Bone-china ceramic powder and granite industrial by-product waste in self-compacting concrete: a durability assessment with statistical validation. In: *Structures*. *Els*, vol 54, pp 837–856, nd

Gonzalez-Corominas A, Etxeberria M (2014) Properties of high performance concrete made with recycled fine ceramic and coarse mixed aggregates. *Constr Build Mater* 68:618–626. <https://doi.org/10.1016/j.conbuildmat.2014.07.016>

[Article](#) [Google Scholar](#)

Guerra I, Vivar I, Llamas B, Juan A, Moran J (2009) Eco-efficient concretes: the effects of using recycled ceramic material from sanitary installations on the mechanical properties of concrete. *Waste Manag* 29:643–646. <https://doi.org/10.1016/j.wasman.2008.06.018>

[Article](#) [Google Scholar](#)

Guo Y, Zhang T, Tian W, Wei J, Yu Q (2019) Physically and chemically bound chlorides in hydrated cement pastes: a comparison study of the effects of silica fume and metakaolin. *J Mater Sci* 54:2152–2169. <https://doi.org/10.1007/s10853-018-2953-5>

[Article](#) [Google Scholar](#)

Gupta N, Siddique R (2020) Durability characteristics of self-compacting concrete made with copper slag. *Constr Build Mater* 247:118580. <https://doi.org/10.1016/j.conbuildmat.2020.118580>

[Article](#) [Google Scholar](#)

Higashiyama H, Sappakittipakorn M, Sano M, Takahashi O, Tsukuma S (2015) Characteristics of chloride ingress into mortars containing ceramic waste aggregate. *J Mater Cycles Waste Manag* 17:513–521.

<https://doi.org/10.1007/s10163-014-0264-8>

[Article](#) [Google Scholar](#)

Huseien GF, Sam ARM, Shah KW, Mirza J (2020) Effects of ceramic tile powder waste on properties of self-compacted alkali-activated concrete. *Constr Build Mater* 236:117574.

<https://doi.org/10.1016/j.conbuildmat.2019.117574>

[Article](#) [Google Scholar](#)

Jain A, Gupta R, Chaudhary S (2019) Performance of self-compacting concrete comprising granite cutting waste as fine aggregate. *Constr Build Mater* 221:539–552. <https://doi.org/10.1016/j.conbuildmat.2019.06.104>

[Article](#) [Google Scholar](#)

Jain A, Gupta R, Chaudhary S (2020a) Sustainable development of self-compacting concrete by using granite waste and fly ash. *Constr Build Mater* 262:120516.

<https://doi.org/10.1016/j.conbuildmat.2020.120516>

[Article](#) [Google Scholar](#)

Jain A, Siddique S, Gupta T, Sharma RK, Chaudhary S (2020b) Utilization of shredded waste plastic bags to improve impact and abrasion resistance of concrete. *Environ Dev Sustain* 22:337–362.

<https://doi.org/10.1007/s10668-018-0204-1>

[Article](#) [Google Scholar](#)

Jain A, Chaudhary S, Choudhary S, Gupta R (2022a) Resistance of fly ash blended self-compacting concrete incorporating granite powder against acid and sulphate environments. *Arab J Geosci*.

<https://doi.org/10.1007/s12517-022-10424-8>

[Article](#) [Google Scholar](#)

Jain A, Choudhary S, Gupta R, Chaudhary S, Gautam L (2022b) Effect of granite industry waste addition on durability properties of fly ash blended self-compacting concrete. *Constr Build Mater* 340:127727.

<https://doi.org/10.1016/j.conbuildmat.2022.127727>

[Article](#) [Google Scholar](#)

Jerônimo VL, Meira GR, da Silva Filho LCP (2018) Performance of self-compacting concretes with wastes from heavy ceramic industry against corrosion by chlorides. *Constr Build Mater* 169:900–910.

<https://doi.org/10.1016/j.conbuildmat.2018.03.034>

[Article](#) [Google Scholar](#)

Keshavarz Z, Mostofinejad D (2019) Porcelain and red ceramic wastes used as replacements for coarse aggregate in concrete. *Constr Build Mater* 195:218–230. <https://doi.org/10.1016/j.conbuildmat.2018.11.033>

[Article](#) [Google Scholar](#)

Medina C, Frías M, Sánchez De Rojas MI, Thomas C, Polanco JA (2012a) Gas permeability in concrete containing recycled ceramic sanitary ware aggregate. *Constr Build Mater* 37:597–605.

<https://doi.org/10.1016/j.conbuildmat.2012.08.023>

[Article](#) [Google Scholar](#)

Medina C, Sánchez De Rojas MI, Frías M (2012b) Reuse of sanitary ceramic wastes as coarse aggregate in eco-efficient concretes. *Cem Concr Compos* 34:48–54. <https://doi.org/10.1016/j.cemconcomp.2011.08.015>

[Article](#) [Google Scholar](#)

Medina C, Sánchez De Rojas MI, Frías M (2013) Properties of recycled ceramic aggregate concretes: Water resistance. *Cem Concr Compos* 40:21–29. <https://doi.org/10.1016/j.cemconcomp.2013.04.005>

[Article](#) [Google Scholar](#)

Meena RV, Jain JK, Chouhan HS, Beniwal AS (2021) Mechanical and durability performance of self-compacting concrete with waste ceramic tile as a replacement for natural river sand. *Mater Today Proc*.

<https://doi.org/10.1016/j.matpr.2021.12.303>

[Article](#) [Google Scholar](#)

Meena RV, Beniwal AS, Gupta G (2023a) Fresh characteristics and compressive strength evaluation of self-compacting concrete prepared with ceramic waste tile and fly ash. *Mater Today Proc*.

<https://doi.org/10.1016/j.matpr.2023.05.687>

[Article](#) [Google Scholar](#)

Meena RV, Beniwal AS, Jain A, Choudhary R, Mandolia R (2023b) Evaluating resistance of ceramic waste tile self-compacting concrete to sulphuric acid attack. *Constr Build Mater* 393:132042.

<https://doi.org/10.1016/j.conbuildmat.2023.132042>

[Article](#) [Google Scholar](#)

Muniandy R, Ismail DH, Hassim S (2018) Performance of recycled ceramic waste as aggregates in hot mix asphalt (HMA). *J Mater Cycles Waste Manag* 20:844–849. <https://doi.org/10.1007/s10163-017-0645-x>

[Article](#) [Google Scholar](#)

Neville A (2004) The confused world of sulfate attack on concrete. *Cem Concr Res* 34:1275–1296.

<https://doi.org/10.1016/j.cemconres.2004.04.004>

[Article](#) [Google Scholar](#)

Nyunin GI (1984) Means of increasing the acid resistance of porcelain and earthenware. *Glas Ceram* 41:209–211. <https://doi.org/10.1007/BF01159918>

[Article](#) [Google Scholar](#)

Okamura H, Ozawa K, Ouchi M (2000) Self-compacting concrete. *Struct Concr* 2:3–17

[Article](#) [Google Scholar](#)

Rashid K, Razzaq A, Ahmad M, Rashid T, Tariq S (2017) Experimental and analytical selection of sustainable recycled concrete with ceramic waste aggregate. *Constr Build Mater* 154:829–840.

<https://doi.org/10.1016/j.conbuildmat.2017.07.219>

[Article](#) [Google Scholar](#)

Rilem RDEL, Matt T (1988) TC56–MHM HYDROCARBON MATERIALS CPC–18 Measurement of hardened concrete carbonation depth 2, 2–4

Rubio F, Rubio J, Oteo JL (1997) A DSC study of the drying process of TEOS derived wet silica gels.

*Thermochim Acta* 307:51–56. [https://doi.org/10.1016/S0040-6031\(97\)00309-2](https://doi.org/10.1016/S0040-6031(97)00309-2)

[Article](#) [Google Scholar](#)

Siddique S, Shrivastava S, Chaudhary S (2017) Lateral force microscopic examination of interfacial transition zone in ceramic concrete. *Constr Build Mater* 155:688–725.

<https://doi.org/10.1016/j.conbuildmat.2017.08.080>

[Article](#) [Google Scholar](#)

Siddique S, Shrivastava S, Chaudhary S (2018a) Durability properties of bone china ceramic fine aggregate concrete. *Constr Build Mater* 173:323–331. <https://doi.org/10.1016/j.conbuildmat.2018.03.262>

[Article](#) [Google Scholar](#)

Siddique S, Shrivastava S, Chaudhary S (2018b) Evaluating resistance of fine bone china ceramic aggregate concrete to sulphate attack. *Constr Build Mater* 186:826–832.

<https://doi.org/10.1016/j.conbuildmat.2018.07.138>

[Article](#) [Google Scholar](#)

Siddique S, Shrivastava S, Chaudhary S, Gupta T (2018c) Strength and impact resistance properties of concrete containing fine bone china ceramic aggregate. *Constr Build Mater* 169:289–298.

<https://doi.org/10.1016/j.conbuildmat.2018.02.213>

[Article](#) [Google Scholar](#)

Siddique S, Chaudhary S, Shrivastava S, Gupta T (2019) Sustainable utilisation of ceramic waste in concrete: exposure to adverse conditions. *J Clean Prod* 210:246–255. <https://doi.org/10.1016/j.jclepro.2018.10.231>

[Article](#) [Google Scholar](#)

Siddique S, Gupta T, Thakare AA, Gupta V, Chaudhary S (2021) Acid resistance of fine bone china ceramic aggregate concrete. *Eur J Environ Civ Eng* 25:1219–1232. <https://doi.org/10.1080/19648189.2019.1572543>

[Article](#) [Google Scholar](#)

Števíla L, Madej J, Kozánková J, Madejová J (1994) Hydration products at the blastfurnace slag aggregate—cement paste interface. *Cem Concr Res* 24:413–423. [https://doi.org/10.1016/0008-8846\(94\)90128-7](https://doi.org/10.1016/0008-8846(94)90128-7)

[Article](#) [Google Scholar](#)

Suzuki M, Seddik Meddah M, Sato R (2009) Use of porous ceramic waste aggregates for internal curing of high-performance concrete. *Cem Concr Res* 39:373–381. <https://doi.org/10.1016/j.cemconres.2009.01.007>

[Article](#) [Google Scholar](#)

Vilas R, Kumar J, Singh A (2022a) Sustainable self-compacting concrete containing waste ceramic tile aggregates: fresh, mechanical, durability, and microstructural properties. *J Build Eng* 57:104941

[Article](#) [Google Scholar](#)

Vilas R, Kumar J, Singh H, Singh A (2022b) Use of waste ceramics to produce sustainable concrete: a review. *Clean Mater*. <https://doi.org/10.1016/j.clema.2022.100085>

[Article](#) [Google Scholar](#)

Vilas Meena R, Kumar Jain J, Singh Chouhan H, Mandolia R, Singh Beniwal A (2021) Impact of waste ceramic tile on resistance to fire and abrasion of self-compacting concrete. *Mater Today Proc*.

<https://doi.org/10.1016/j.matpr.2021.12.287>

[Article](#) [Google Scholar](#)

## Author information

---

### Authors and Affiliations

Department of Civil Engineering, JECRC University, Jaipur, 303905, India

Ram Vilas Meena & Ankit Singh Beniwal

Department of Civil Engineering, Swami Keshvanand Institute of Technology Management and Gramothan, Jaipur, 302017, India

Abhishek Jain

Department of Civil Engineering, Jaipur National University, Jaipur, 302017, India

Om Prakash Singh

Department of Civil Engineering, Manipal University Jaipur, Jaipur, 303007, India

Sanchit Anand

### Contributions

CRedit authorship contribution statement Ram Vilas Meena: Conceptualization, Methodology, Data curation, Investigation, Writing – original draft, Visualization. Abhishek Jain: Visualization, Data curation, Writing – original draft, Writing – review & editing. Ankit Singh Beniwal: Visualization, Investigation, Writing – review & editing. Om Prakash Singh: Writing – review & editing. Sanchit Anand: Writing – review & editing.

### Corresponding authors

Correspondence to [Ram Vilas Meena](#), [Abhishek Jain](#) or [Ankit Singh Beniwal](#).

### Ethics declarations

---

### Competing interests

The authors declare no competing interests.

### Rights and permissions

---

Springer Nature or its licensor (e.g. a society or other partner) holds exclusive rights to this article under a publishing agreement with the author(s) or other rightsholder(s); author self-archiving of the accepted manuscript version of this article is solely governed by the terms of such publishing agreement and applicable law.

[Reprints and permissions](#)

### About this article

---



## Cite this article

Meena, R.V., Jain, A., Beniwal, A.S. *et al.* Performance Evaluation of Self-Compacting Concrete Containing Ceramic Waste Tile Fine Aggregate in Aggressive Environments. *Iran J Sci Technol Trans Civ Eng* **48**, 3955–3970 (2024).

<https://doi.org/10.1007/s40996-024-01346-4>

Received

10 November 2023

Accepted

07 January 2024

Published

03 February 2024

Issue Date

December 2024

DOI

<https://doi.org/10.1007/s40996-024-01346-4>

## Share this article

Anyone you share the following link with will be able to read this content:

[Get shareable link](#)

Provided by the Springer Nature SharedIt content-sharing initiative

## Keywords

[Self-compacting concrete](#)

[Ceramic waste tile aggregate](#)

[Sulphate attack](#)

[Corrosion](#)

[Carbonation](#)

[Fourier transform infrared](#)